A high temperature route to the formation of highly pure quaternary chalcogenide particles

M. Benchikri, Oana Zaberca, Rachida El Ouatib, Bernard Durand, Frédéric Oftinger, Andrea Balocchi, Jean-Yves Chane-Ching

A high temperature route to the formation of highly pure quaternary chalcogenide particles

M. Benchikri [a], O. Zaberca [b], R. El Ouatib [a], B. Durand [b], F. Oftinger [b], A. Balocchi [c], J.Y. Chane–Ching [b,*]

[a] ESCMI, Faculté des sciences d'Ain Chock, Route d'El Jadida, BP 5366 Casablanca, Morocco
[b] Université de Toulouse CNRS-UPS-INPT, CIRIMAT, 118, Route de Narbonne 31062 Toulouse Cedex 9, France
[c] Université de Toulouse, INSA-CNRS-UPS, LPCNO, 135, Avenue de Rangueil, 31077 Toulouse, Cedex, France

A B S T R A C T

A process route to the fabrication of quaternary chalcogenides (Cu_2CoSnS_4, Cu_2ZnSnS_4) particles is proposed in molten KSCN at 400 °C. This high temperature route allows the formation of highly pure and highly crystallized quaternary chalcogenides particles. Control of primary crystallites size is demonstrated by altering the chemical homogeneity of the precursors. This method could be exploited to prepare building blocks for the fabrication of low-cost solar cell absorbers.

Keywords:
Quaternary chalcogenides
Photovoltaics
Particles
Solar cells
Synthesis

1. Introduction

Quaternary chalcogenides (Cu_2CoSnS_4, Cu_2ZnSnS_4) materials have been of interest for many years because they possess suitable direct band gap and high absorption coefficient for application in solar energy conversion [1,2]. These materials have recently attracted increased attention for photovoltaic conversion since there are composed of only abundant non-toxic elements. Cu_2ZnSnS_4 (CZTS) is thus considered as a promising material for low cost absorber layer for solar cells [3]. Extensive pioneering work on this material employing evaporation based approach under vacuum was performed by the group of Prof. Katagiri [4,5]. Using RF co-sputtering of Cu and binary ZnS and SnS materials, a 6.77% efficient solar cell was demonstrated in 2008 [5]. More recently, efficiency of quaternary chalcogenides based solar cells via an ink printing process route involving the use of nanosized Cu_2ZnSnS_4 building blocks has been recently reported up to 9.66% [6]. Indeed, direct liquid deposition approaches are particularly attractive for large scale manufacturing due to their compatibility with high throughput deposition techniques such as tape casting. Various processing routes have already been proposed for the preparation of Cu_2ZnSnS_4 particles [7,8,9,10]. These routes involve the use of coordinating solvent such as oleyl-amine or surfactants and are performed at synthetic temperatures ranging from 225 °C to 300 °C. Because defects usually act as hole/electron recombination centers during the photovoltaic conversion, the development of new process routes allowing the preparation of highly crystallized quaternary chalcogenides particles is of great interest [11] since these materials should exhibit lower defect concentration.

Here we report on a high temperature route (T = 400 °C) to the formation of highly crystallized quaternary chalcogenides building blocks involving direct reactions between metal oxides or metallic salts precursors in molten KSCN.

2. Experimental section

Preparation of quaternary chalcogenides in molten KSCN was investigated using two different procedures. A first procedure involves metal oxides as metal sources: SnO_2 (Acros), ZnO or CoO (Acros), Cu_2O (Aldrich). The metal oxides were used as-received without any post milling stage in order to avoid any impurity contamination. These metal oxide raw materials consist of aggregates possessing various aggregate sizes in the micronic range as determined from SEM: 20 μm (SnO_2), 5 μm (Cu_2O), 2 μm (CoO), 1 μm (ZnO). A solid precursor, denoted oxide precursor was prepared by intimate mixing performed in a solid vortex mixer (Top Mix, Fisher Scientific) of these metal oxide aggregates with solid KSCN, (Sigma-Aldrich > 99%). With the objective to improve the chemical homogeneity of the solid precursors, a modified procedure involves in a first stage a SnO_2 (or SnO_2-$M(OH)_2$, M = Co, Zn)–Cu_2O intimate mixture prepared from roto-evaporation at 80 °C under vacuum of a ethanolic dispersion formed from a precipitated SnO_2 or co-precipitated SnO_2–$M(OH)_2$ with Cu_2O particles. In a second stage, a homogeneous oxide precursor was achieved by mixing in a solid vortex mixer of this freshly prepared SnO_2 (or co-precipitated SnO_2–$M(OH)_2$)–Cu_2O mixture with solid KSCN.

* Corresponding author.
E-mail address: chane@chimie.ups-tlse.fr (J.Y. Chane–Ching).

Similarly, in a second procedure, a salt precursor was prepared by intimate mixing using the same solid vortex mixer of metallic salts as metal sources: $SnCl_4$ $5H_2O$ (Fisher Scientific), CuCl 2 H_2O (Sigma Aldrich), $ZnCl_2$ (Sigma Aldrich) and solid KSCN. For these two procedures, the precursors were transferred into an alumina crucible and post heat treated under N_2 controlled atmosphere. Reaction mixtures were maintained at various temperatures ranging from T = 300 °C to 550 °C with various duration times t (3 h<t<48 h). After cooling at room temperature, the black CZTS powder was separated and collected from excess KSCN by subsequent washings in deionized water, EtOH and finally dried at room temperature in air.

The resulting CZTS samples were characterized by SEM (JEOL JSM-6510), XRD (Brucker AXS D4) and Raman Spectroscopy. Raman spectroscopy was performed on washed, dried solid samples using a Horiba Jobin Yvon XPlora spectrometer with λ = 633 nm at a laser power P = 1.7 mW.

3. Results and discussion

Preliminary experiments were performed using oxide precursors with $(Cu: M: Sn: S)_{moles} = (2: 1: 1: S)$ compositions, where S denotes the number of KSCN moles and M = Zn or Co. Formation of the desired quaternary chalcogenide structures was observed in the temperature range 350 °C<T<500 °C. At a too low temperature, T = 300 °C, XRD patterns (not shown) revealed incomplete transformation of the oxide raw materials. In a typical experiment, oxide precursors with an optimal KSCN composition $(Cu: M: Sn: S)_{molar\ ratio} = (2: 1: 1: 15)$ were heat treated at 400 °C during 24 h. Corresponding X-Ray diffraction patterns of Cu_2CoSnS_4 (CCTS) and Cu_2ZnSnS_4 (CZTS) samples (Fig. 1) exhibit peaks corresponding to the quaternary chalcogenide quadratic phase. Indeed, fine inspection of the diffractogramms recorded on CCTS samples reveals the presence of SnO_2 and Co_3S_4 as minor structures. Because the corresponding oxide metal sources were incorporated in the reaction mixture as large micronic particles, improvement of precursors chemical homogeneity was investigated with the objective to prepare samples exhibiting a single quaternary chalcogenide quadratic phase. Thus, more homogeneous precursors involving precipitated SnO_2 or co-precipitated SnO_2–$Co(OH)_2$ were investigated. Corresponding XRD patterns of the resulting oxide precursors after heat treatment in similar conditions of temperature and duration as previously described

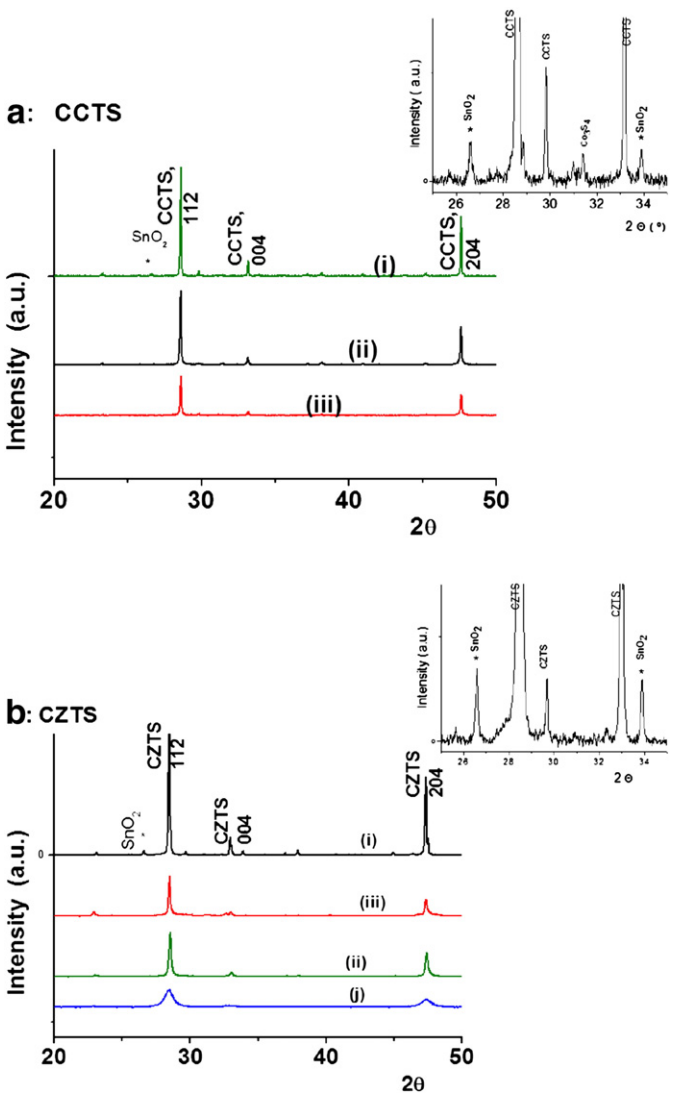

Fig. 1. X-Ray diffractogramms showing formation of pure quaternary chalcogenide prepared at T = 400 °C during 24 h. (a) CCTS curve i: Cu_2O, CoO, SnO_2, KSCN. Curve ii: Cu_2O, CoO, precipitated SnO_2, KSCN. curve iii: Cu_2O, co-precipitated $Co(OH)_2$ -SnO_2, KSCN. (b) CZTS. Curve i: Cu_2O, ZnO, SnO_2, KSCN. Curve ii: Cu_2O, ZnO, precipitated SnO_2, KSCN. Curve iii: Cu_2O, co- precipitated $Zn(OH)_2$ -SnO_2, KSCN. Curve j: CuCl, $ZnCl_2$, $SnCl_4$ $5H_2O$ KSCN. * indicates peaks assigned to SnO_2 Inserts: curves (i), 2θ = 25–35°.

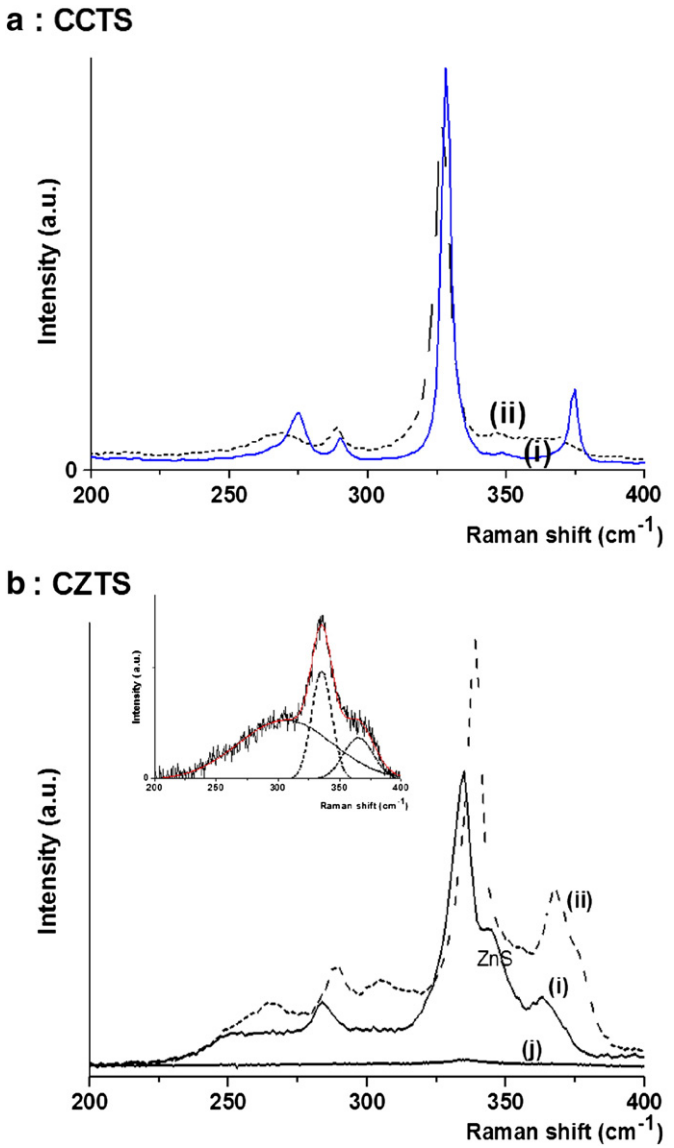

Fig. 2. Raman spectra of (a) CCTS crystals: curve (i) Cu_2O, CoO, SnO_2, KSCN. curve (ii) Cu_2O, CoO, precipitated SnO_2, KSCN. (b) CZTS crystals: curve (i) Cu_2O, ZnO, SnO_2, KSCN. Curve (ii) Cu_2O, ZnO, precipitated SnO_2, KSCN. Curve (j) $CuCl_2$, $ZnCl_2$, $SnCl_4$ $5H_2O$, KSCN. Insert: deconvolution of curve j showing peaks assigned to CZTS.

Table 1
XRD and Raman characteristics of CCTS and CZTS samples prepared from oxide and salt precursors. d_{XRD} denotes the ordered domain size determined from Scherrer equation. Peak #1 characteristics refer to main peak of the Raman spectrum. Reported Raman shift (ν), and FWHM (w) values of the various peaks were determined after deconvolution of the Raman spectra between 250 and 400 cm^{-1}.

		XRD	Raman							
			# 1		#2		#3		# 4	
		d_{XRD} (nm)	ν_1 (cm^{-1})	w_1 (cm^{-1})	ν_2 (cm^{-1})	w_2 (cm^{-1})	ν_3 (cm^{-1})	w_3 (cm^{-1})	ν_4 (cm^{-1})	w_4 (cm^{-1})
CCTS	Oxides	>250	328	4	290	4	374	35		
	Precip. SnO_2	240	326	6.5	288	5	359	27		
CZTS	Oxides	250	334	9	305	95	361	14	346	7
	Precip. SnO_2	60	335	15	304	81	365	19		
	Salts	12	335	16	306	87	365	24		

show a single CCTS phase confirming effect of chemical homogeneity of the precursors on the preparation of highly pure CCTS in molten KSCN.

Similar to the formation of CCTS, the CZTS XRD patterns reveal presence of SnO_2 structure as a minor constituent. Using the same modified procedure, preparation of samples exhibiting a single CZTS phase was achieved via a mixture involving use of a freshly precipitated SnO_2 intimately mixed to Cu_2O and ZnO particles.

In addition to the XRD, Raman investigation was performed to fully characterize the samples. Indeed, Raman characterization is crucial to complete CZTS structure identification since XRD does not allow the distinction between the CZTS and ZnS, Cu_2SnS_3 structures. As an example, a peak was observed at 345 cm^{-1} indicating presence of cubic ZnS [12] for the CZTS sample prepared from an oxide precursor involving Cu_2O, SnO_2, ZnO and KSCN as raw materials (Fig. 2). In contrast, by improving the chemical homogeneity of the oxide precursor using the modified procedure, Raman spectrum of the resulting sample shows a main peak at 335 cm^{-1} and secondary peaks at 286 and 361 cm^{-1} [13] attributed to the CZTS structure.

The Raman spectra recorded on CCTS samples show a slight variation of the main peak frequency determined at 326 cm^{-1} with secondary peaks at 288 cm^{-1} and 359 cm^{-1}. Indeed, although no reference to the best of our knowledge has been published concerning CCTS, these peaks are consistent with the totally symmetric vibration involving the motion of sulfur atoms of quaternary chalcogenides [13] and could be attributed to CCTS. More important, the high value of the primary crystallite determined by XRD is consistent with the low value of the FWHM determined from the Raman spectra of the CCTS and CZTS samples (Table 1) and indicates the formation of highly crystallized quaternary chalcogenides particles in molten KSCN at 400 °C.

Indeed, XRD and Raman data reveal large differences concerning the CCTS and the CZTS formation from oxide raw materials in molten

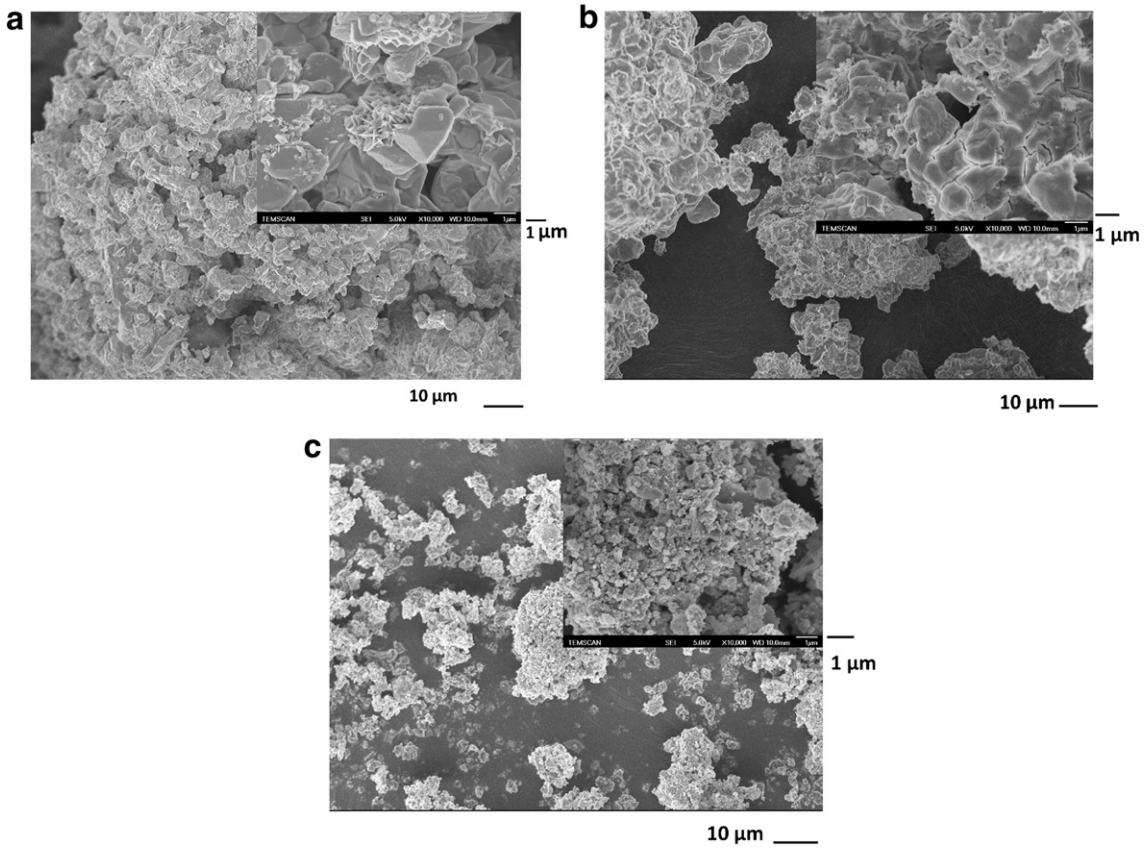

Fig. 3. Morphology of quaternary chalcogenides particles prepared in molten KSCN at 400 °C (a) CCTS particles, Cu_2O–CoO–SnO_2–KSCN precursor. (b) CZTS particles Cu_2O–ZnO–SnO_2–KSCN precursor, (c) CZTS particles, CuCl–$ZnCl_2$–$SnCl_4$ 5 H_2O–KSCN precursor. Scale Bar = 10 µm. Insert: High magnification images. Scale Bar = 1 µm.

KSCN. In contrast to the formation of CCTS particles which occurs without cobalt sulfide phase, formation of non-desired ZnS was observed during the CZTS synthesis although using ZnO raw material of slighter small particle size compared to CoO. In addition, larger primary crystallite sizes as calculated from the Scherrer equation (Table 1), consistent with the lower FWHM values of the main Raman peak were determined for CCTS particles (Table 1). In addition, compared to bulk CZTS, unexplained large FWHM values of the secondary Raman peak centered around 305 cm^{-1} were determined on CZTS samples. All these observations suggest an easier formation of the CCTS quaternary chalcogenide structure in comparison to CZTS.

SEM observation of the as-synthesized samples (Fig. 3) indicates that the quaternary chalcogenides particles are indeed of micronic size and largely aggregated with a polydisperse size distribution. High magnification images show that these particles are composed of primary crystallites possessing sizes larger than 1 μm.

Interestingly, our data clearly show large variation in primary crystallite size of the CZTS crystals. Because the chemical homogeneity of the various components into the precursors was shown to greatly affect the primary crystallite size and probably the nucleation rate of the quaternary chalcogenide particles, we have investigated preparation of CZTS particles from precursors made from metallic salts. In a typical experiment, an intimate mixture of the various metallic salts and KSCN with (Cu: Zn: Sn: S = (2: 1: 1: 15) composition was heat treated at T = 400 °C for 16 h. XRD and Raman spectra performed on samples synthesized at temperature of 400 °C and duration time of 16 h demonstrated that the resulting product can be fully identified as a pure CZTS compound. As expected, particles prepared from salts precursors exhibit smaller primary crystallite sizes of around 12 nm, as calculated from the Scherrer equation using the full-width at the half-maximum of the chalcogenide (112) XRD peak. Consistently, the FWHM of the main peak of the Raman spectra (FWHM = 16 cm^{-1}) display a higher value indicating a lower short range order compared with the samples synthesized from the oxide precursors. High magnification SEM images confirm the presence of smaller size of primary crystallites compared with samples synthesized using an oxide precursor. Nevertheless, these primary crystallites are fully aggregated with size in the micronic range exhibiting non-well defined morphology.

Depending on the precursors, various mechanisms have been already proposed for the formation of the metallic sulfide particles in molten KSCN. Thermal decomposition of KSCN starts at 275 °C [14] with S formation: $SCN^- = S + CN^-$. Using oxide precursors, formation of the quaternary chalcogenides is achieved with the following reaction: $Cu_2O + ZnO + SnO_2 + 4\ KSCN = Cu_2ZnSnS_4 + 4\ KCNO$ [15]. In contrast, formation of the quaternary chalcogenides from metallic salts probably involves the following steps [15]: i/ $S + 2\ CN^- = S^{2-} + C + N_2$ or $S + 2\ CN^- = S^{2-} + C + N_2$ ii/ $2\ Cu^+ + Zn^{2+} + Sn^{2+} + 4\ S^{2-} = Cu_2ZnSnS_4$. The lower crystallite sizes determined on samples prepared from salt precursors suggest a higher nucleation rate for the formation of the quaternary chalcogenides. This higher nucleation rate probably arises from the high concentration of directly available metallic cations in the molten KSCN.

4. Conclusions

A high temperature route to the formation of pure, highly crystallized quaternary chalcogenide (Cu_2CoZnS_4, Cu_2ZnSnS_4) particles is proposed in molten KSCN at 400 °C. We demonstrated the crucial role of the chemical homogeneity of the various Cu_2O–MO–(M = Zn or Co) –SnO_2–KSCN precursors in order to achieve a pure quaternary chalcogenide structure. The chemical homogeneity of the precursors was also shown to greatly affect the nucleation rate of the quaternary chalcogenide particles. Smallest primary crystallite sizes were thus achieved using a salt precursor (CuCl–$ZnCl_2$–$SnCl_4$ $5H_2O$–KSCN) promoting a high nucleation rate regime probably resulting from directly available metallic cations. These results thus highlight the ability to synthesize highly pure and highly crystallized CZTS particles with controlled primary crystallite sizes.

Acknowledgements

This work was supported by two French-Moroccan projects: Volubilis Partenariat Hubert Curien (PHC No. MA 09 205)" and Projet de Recherches sur Convention Internationale du CNRS (CNRS-CNRST No. w22572).

References

[1] Ito K, Nakazawa T. Jpn J Appl Phys 1988;27:2094–7.
[2] Seol JS, Lee SY, Lee JC, Nam HD, Kim KH. Sol Energy Mater Sol Cells 2003;75:155–62.
[3] Scragg JJ, Dale PJ, Peter L, Zoppi G, Forbes I. Phys Status Solidi B 2008;245(9):1772–8.
[4] Katagiri H, Sasaguchi N, Hando S, Hoshino S, Ohashi J, Yokota T. Sol Energy Mater Sol Cells 1997;49:407–14.
[5] Katagiri H, Jimbo K, Yamada S, Kamimura Y, Maw WS, Fukano T, et al. Appl Phys Express 2008;1:041201–2.
[6] Todorov TK, Reuter KB, Mitzi DB. Adv Mater 2010;22:1–4.
[7] Guo O, Hillhouse HW, Agrawal R. J Am Chem Soc 2009;131:11672–3.
[8] Riha SC, Parkinson BA, Prieto AL. J Am Chem Soc 2009;131:12054–5.
[9] Steinhagen C, Panthani MG, Akhavan V, Goodfellow B, Koo B, Korgel BA. J Am Chem Soc 2009;131:12554–5.
[10] Shavel A, Arbiol J, Cabot A. J Am Chem Soc 2010;132:4514–5.
[11] Chane-Ching JY, Gillorin A, Zaberca O, Balocchi A, Marie X. Chem Commun 2011;47:5229–31.
[12] Xu ZY, Zhang YC. Mater Chem Phys 2008;112:333–6.
[13] Himmrich M, Haeusler H. Spectrochim Acta 1991;47 A(7):933–42.
[14] Eluard A, Tremillon B. J Electroanal Chem 1967;13:208–26.
[15] Bohac P, Tanner V, Gaeumann A. Cryst Res Technol 1982;17:717–22.